Waste Management 138 (2022) 298–307

Contents lists available at ScienceDirect

Waste Management

journal homepage: www.elsevier.com/locate/wasman

Effect of pretreatment and biomass blending on bio-oil and biochar quality from two-step slow pyrolysis of rice straw

Anubhuti Bhatnagar *, Abhishek Singhal, Henrik Tolvanen, Kati Valtonen, Tero Joronen, Jukka Konttinen

Tampere University, Faculty of Engineering and Natural Sciences, Materials Science and Environmental Engineering, Korkeakoulunkatu 8, FI-33720 Tampere, Finland

ARTICLE INFO

Keywords:
TGA
Kinetic coefficients
Levoglucosan
Ash elements
Washing
Co-pyrolysis

ABSTRACT

This study investigated biomass blending and water washing to improve product quality from two-step pyrolysis of rice straw. Rice straw (RS) was mixed with groundnut shells (GNS) and wheat straw (WS) in different weight ratios. Blending RS with GNS/WS in a 1:1 ratio increased the total bio-oil yields by 7–9% and reduced the pyrolysis gas and char yields by 5–7% and < 2%, respectively. RS was washed with water separately to examine the effect of removing water-soluble ash elements. The optimum washing duration was 60 min; the ash removal efficiency was then 26%. The bio-oil yields from washed straw increased by 4% over unwashed straw, and pyrolysis gas yields decreased. Combining the washing and blending processes increased the levoglucosan yield by 1.6–2.1 times compared to unwashed RS, and the water content in bio-oil was reduced by ~ 10%.

Moreover, the biochar samples obtained after pyrolysis of washed biomass blends had potential fuel applications owing to low fouling or slagging propensity. They also had possible use in the soil for adsorption of soil contaminants and increasing acidic soil pH, with likely stability of ~ 1000 years in the ground. These results provide a promising alternative for efficiently converting rice straw to multiple value-added products.

1. Introduction

Rice straw is a potential feedstock in the bio-economy since rice is among the most important grain crops globally, with production reaching 755.5 million tons (MT) in 2019 (FAO, 2021). China (211.4 MT) and India (177.6 MT) account for 51.5% of the total production (FAO, 2021). The straw-to-grain proportion of rice ranges from 0.7 to 1.4 (Directorate of Economics & Statistics, 2020). Thus, 600–1000 MT of rice straw is produced globally every year, with about 90% produced in Asia. However, in India, due to the low bulk density of straw, short collection time between cropping cycles, and poor transportation infrastructure, these residues are burnt in open fields (Singh et al., 2021).

Integrated biorefineries that combine decentralized pyrolysis and centralized refinement of bio-oil have been proposed as a solution. A decentralized unit may treat straw on-farm site, and bio-oil (denser than rice straw) may be transported to a refinery for chemical production (Fytili and Zabaniotou, 2018). Evaluating pyrolysis-based biorefineries using rice straw is also essential due to the prospect of producing both bio-oil and biochar. Bio-oil is an excellent chemical feedstock for fine and platform chemicals (Mohan et al., 2006), while biochar can be used as a fuel or adsorbent or enhance soil productivity (Klinar, 2016).

A challenge for the pyrolysis of rice straw is its high ash content (up to 18%), which comprises primarily of alkaline and alkaline earth metals (AAEMs) and silica (Raveendran et al., 1995). AAEMs heterogeneously catalyze vapor-phase reactions, promoting pyrolysis gases over bio-oil (Huang et al., 2020). The catalytic effects of these AAEMs have been reviewed in great detail by Wang et al. (2017) to provide insights into the interaction between biopolymers and AAEMs during pyrolysis. Specifically, Na and K catalyze levoglucosan cracking via dehydration reactions (Eom et al., 2013), which is undesirable since it is a high-value chemical. K also reduces selectivity toward monophenols (one hydroxyl group on an aromatic ring) and increases selectivity toward polyphenols (multiple hydroxyl groups on an aromatic ring) and short-chain aldehydes (Zhang et al., 2017). Mg and Ca, which are strong Lewis acids, increase the dehydration of cellulose, forming furfural (Li et al., 2020). Polyphenols, short-chain aldehydes, and other products of dehydration reactions are highly reactive and change the properties of bio-oil over time. This process is called “aging” (Czernik et al., 1994), which results in increased bio-oil viscosity and water content and reduced yields of

* Corresponding author.
E-mail address: anubhutibhatnagar@tuni.fi (A. Bhatnagar).

https://doi.org/10.1016/j.wasman.2021.12.013
Received 7 September 2021; Received in revised form 1 December 2021; Accepted 7 December 2021
Available online 15 December 2021

value-added chemicals.

Furthermore, over 95% of all ash content is sequestered in the char after pyrolysis (Leijenhorst et al., 2016), which reduces the calorific value and the adsorption capacity of biochar (Ghodake et al., 2021). Therefore, reducing the ash content in rice straw can significantly improve the quality of both bio-oil and biochar.

In the past decade, multiple research studies have explored the alteration of pyrolysis pathways to enhance the production of value-added chemicals (e.g., levoglucosan and vanillin) and minimize the formation of low-quality products, such as pyrolysis gases. One of these pathways is stepwise pyrolysis, which involves heating the feedstock in discrete temperature steps to achieve a gradual release of volatiles and the collection of bio-oil in separate fractions (de Wild et al., 2009). Stepwise pyrolysis exploits the differences in the thermochemical stability of biopolymers (hemicellulose, cellulose, and lignin). Hemicellulose breaks down between 200 °C and 300 °C to form acetic acid, furfural, and hydroxyacetaldehyde (Peng et al., 2012). Cellulose breaks down between 280 °C and 400 °C to give anhydrosugars and oligosaccharides (Caballero et al., 1997). Lignin depolymerizes gradually between 200 °C and 900 °C to yield substituted phenols such as guaiacol, syringol, and catechol (Mante et al., 2016). Bhatnagar et al. (2020) reported that two-step pyrolysis of rice straw enhanced the separation of organic acids, anhydrosugars, and carbonyl compounds from unbranched phenolic compounds, reducing the complexity of bio-oil. This separation ensured that bio-oil was more stable over four weeks than bio-oil obtained in a single step (Bhatnagar et al., 2021). In a preliminary economic assessment, Bhatnagar et al.(2020) also estimated that the cumulative value of bio-oil from two-step pyrolysis was 2–2.5 times higher than that of bio-oil from single-step pyrolysis for crop residues.

This study used two-step heating in combination with pretreatment and co-pyrolysis to further reduce the impact of rice straw ash content on the quality of bio-oil and biochar. An overview of recent studies using these strategies is provided in Table S1. These studies have shown that incorporating tires (Alvarez et al., 2019), coal blends (He et al., 2018), and synthetic polymers (Özsin and Pütün, 2018) into biomass improves the aromatic content and stability of bio-oil while decreasing its oxygen content. Chen et al. (2017) also reported the co-pyrolysis of bamboo and microalgae (*Nannochloropsis* sp.). The bio-oil yield was 61 wt% in samples without microalgae and 66.6 wt% in samples with microalgae. Notably, the content of long-chain fatty acids in bio-oil obtained from samples with microalgae was up to 50.9% higher than that obtained from samples without microalgae. Abnisa and Wan Daud (2014) reviewed biomass co-pyrolysis as a method for improving bio-oil quality and found that the success or failure of co-pyrolysis depended on the extent to which the blended feedstock influenced the pyrolytic reactions. In the case of rice straw, co-pyrolysis with locally abundant crop residues has not been sufficiently explored despite its practical relevance. Two such residues that could be used are wheat straw and groundnut shells since they grow in the same regions as rice straw. Besides, India's annual wheat straw production is 110 MT, while groundnut shell is 12 MT (Devi et al., 2017), making them abundantly available. The ash content in these residues is 4–9% (Raveendran et al., 1995). Their availability and composition suggest their suitability for co-pyrolysis with rice straw in a decentralized biorefinery.

Furthermore, biomass washing with acids (HF, HNO_3, and acetic acid) or water also reduces the concentration of AAEMs (Eom et al., 2013; Mourant et al., 2011; Singhal et al., 2021; Zhang et al., 2017). These inorganic elements are present in biomass as water-soluble ions (Na^+, K^+, Ca^{2+}, Mg^{2+}) in biomass fluids or covalently bonded with the organic biomass structure (SO_4^{2-} and PO_4^{3-}). It has been shown that washing with water for 10–15 min reduces the K content in wheat straw (Singhal et al., 2021) and rice husk (Bandara et al., 2020) by > 50%. Further reduction in AAEMs can be achieved by washing with inorganic acids (Eom et al., 2013) and the acetic acid-rich aqueous phase of bio-oil (Chen et al., 2019). Eom et al. (2013) reported that washing rice straw with 3% HF at 30 °C for 1 h reduced the ash content from 9.7% to 0.64%. As shown in Table S1, acid-washing reduces the biochar yields and increases the bio-oil yields. Dilute acid washing of macroalgae (*Enteromorpha clathrata*) prevents the formation of oxygenated chemicals and acids in bio-oil due to the removal of Ca (Cao et al., 2019) and also improves the bio-oil yield from torrefied biomass (Zhang et al., 2018). Water washing before torrefaction can be used to improve the combustion properties of straw and grass-like biomasses (Abelha et al., 2019). Although, acid leaching provides higher bio-oil and sugar yields from biomasses than water washing (Chen et al., 2019; Wang et al., 2021), it is more energy and resource-intensive than water washing due to the requirement of biomass neutralization before pyrolysis and treating acidic wastewater generated in the process. Therefore, in a scenario with limited resource availability, such as a decentralized pyrolysis unit in India, water-washing of rice straw can be more easily optimized than acid-washing.

Although the specific effects of co-pyrolysis and washing on improving pyrolysis product quality by reducing the ash content have been reported, their integrated effect on the two-step pyrolysis of biomass has not been investigated. Since two-step pyrolysis is an effective method for pyrolyzing residues while minimizing the effect of ash on bio-oil composition, it is crucial to fill this knowledge gap. Two-step pyrolysis has an additional advantage for a decentralized unit since the operational requirements for residue management on farms are reduced by controlling the pyrolysis temperature rather than including temperature-controlled condenser units. Hence, this work investigated the effects of the co-pyrolysis of rice straw with groundnut shells and wheat straw before and after water washing on pyrolysis kinetics, product yields, and bio-oil and biochar compositions. The results can help valorize rice straw to make multiple value-added products while preventing open burning.

2. Material and methods

2.1. Biomass source characterization

Rice straw (RS), groundnut shells (GNS), and wheat straw (WS) samples were provided by Valmet Technologies Oyj, Finland. These samples were shredded and sieved to a particle size of 0.2 mm for composition analysis. ASTM standards were used for estimating the moisture (ASTM E1358), volatile (ASTM E872), and ash (ASTM E1755) content in biomass, and fixed carbon was calculated by difference. The CHNS/O content of oven-dried (at 105℃ for 2 h) biomass samples was assessed using a Thermo Scientific™ Flash Smart™ Elemental Analyzer with a thermal conductivity detector. The gross calorific value (GCV) was obtained from the composition (Channiwala and Parikh, 2002).

The ash composition was estimated using inductively coupled plasma mass spectrometry (ICP-MS, Thermo Scientific™ iCAP™ RQ). Dried biomass (0.5 g) was heated in a muffle furnace at 600 °C for 2 h, and the obtained ash was digested with 10 ml of ultrapure concentrated HNO_3 (65% solution) and 1 ml HF (38% solution) before analysis. A detailed method is provided in Bhatnagar et al. (2021).

2.2. Optimizing co-pyrolysis and washing pretreatment

Rice straw was mixed with WS and GNS separately in the proportion of 1:1, 1:2, 1:3 (w/w) to determine the optimum mixing ratio (particle size: 0.2 mm). The composition of the blended biomass was analyzed using methods described in Section 2.1. Thermogravimetric analysis (TGA) was performed for individual biomasses and their blends. The synergistic effect (%) of GNS and WS on RS was determined by calculating the deviations of the observed behavior of the blends from the predicted behaviors using Equations (1) and (2).

$$P_{Pred} = x_{RS} \times P_{RS} + x_{GNS/WS} \times P_{GNS/WS} \quad (1)$$

$$Synergisticeffect(\%) = P_{Obs} - P_{Pred} \quad (2)$$

Here, P_{Obs} is any observed property of the blended sample, and P_{Pred} is the predicted value of the blended sample, x_{RS} and $x_{GNS/WS}$ indicate the fraction of RS, GNS, and WS in the blended sample, and P_{RS} and $P_{GNS/WS}$ are the observed values for individual RS, GNS, and WS samples. The synergistic effect refers to the influence of mixing two biomasses, and a positive value implies the observed values were higher than predicted.

The RS samples (0.2 mm size) were washed for 30, 60, and 120 min in another set of experiments. Each washing experiment was performed twice. Approximately 2 g of RS samples and deionized water were added to air-tight glass bottles (RS to water = 1:20). The samples were placed in an incubator shaker and heated to 40 °C at 100 rpm. Afterward, the leachate was separated from the washed feedstock, and the wet samples were squeezed to remove residual water. Then, samples were oven-dried at 65 °C for 12 h and stored overnight before weighing. Lower drying temperature was chosen to prevent the loss of volatiles before mass yields were calculated. The detailed washing procedure is described in (Singhal et al., 2021). The effect of washing was determined from sample composition (methods described in Section 2.1), TGA, mass yields (Equation (3)), and removal efficiency of ash content and AAEMs (Equation (4)).

$$\text{Massyields}(\%) = \left(\frac{m_w \times R_w}{m_o \times R_o}\right) \times 100\% \tag{3}$$

$$\text{Removalefficiency}(\%) = \left(1 - \frac{m_w \times R_w}{m_o \times R_o}\right) \times 100\% \tag{4}$$

Here, $m_o$is the weight of the unwashed sample, $m_w$is the weight of the sample after washing, $R_o$is the ash or AAEM content in unwashed sample and R_w is the ash or AAEM content in the washed sample.

Both GNS and WS were washed for the optimized time (as per results of RS washing) before blending with RS in the optimized ratio to evaluate the combined effects of pretreatment with co-pyrolysis in the batch reactor study using stepwise heating (see Section 2.4).

2.3. Thermogravimetric analysis and non-isothermal kinetic analysis

Thermogravimetric analysis (TGA) was performed to evaluate the effects of each treatment strategy on the thermal breakdown of rice straw, and the results were used for non-isothermal kinetic analysis. TGA of unwashed RS samples, RS–GNS blends, RS–WS blends, and washed RS samples was performed using 20 mg samples in a Linseis Simultaneous Thermogravimetric Analyzer (PT1600). Oven-dried (105 °C for 2 h) samples were heated during TGA from 20 °C to 600 °C at 5 °C/min with N_2 purge gas (200 ml/ min). The influence of co-pyrolysis and washing on volatile release was compared using the devolatilization index or D_i (Equation (5)).

$$D_i\left(wt\%min^{-2} \circ C^{-3}\right) = \frac{DTG_{peak} \times DTG_{mean}}{T_i T_{peak} \Delta T_{1/2}} \tag{5}$$

Here, DTG_{peak} is the maximum mass loss rate (wt%/min), DTG_{mean} (wt %/ min) is the mean mass loss over the entire duration of analysis, T_i(°C) is the pyrolysis onset temperature, T_{peak} (°C) is the temperature of DTG_{peak}, and $\Delta T_{1/2}$ (°C) is the temperature interval when DTG/DTG_{peak} equals ½.

The non-isothermal kinetic analysis for each case was performed using Coats–Redfern methods (Equations (6) and (7)). The detailed derivation of the equation is shown (Cai and Bi, 2008).

$$\lg\left(\frac{1-(1-\alpha)^{1-n}}{T^2(1-n)}\right) = \lg\frac{AR}{\beta E_a} - \frac{E_a}{2.3RT} \text{for} n \neq 1 \tag{6}$$

$$\lg\left(-\frac{ln(1-\alpha)}{T^2}\right) = \lg\frac{AR}{\beta E_a} - \frac{E_a}{2.3RT} \text{for} n = 1 \tag{7}$$

Here, $f(\alpha)$ is a function associated with the pyrolysis reaction model. The conversion (α) of the samples was $\frac{w_0 - w}{w_0 - w_f}$, where w_0 is the initial weight, w is the weight at any instant during the reaction, and w_f is the terminal weight of samples. For a constant heating rate β (K/min), A is a pre-exponential factor (min^{-1}), E_a is the apparent activation energy (kJ/ mol), R is the gas constant (8.314 J/ mol/K), and T is the absolute temperature (K). A plot of $\lg\left(\frac{1-(1-\alpha)^{1-n}}{T^2(1-n)}\right)$ or $\lg\left(-\frac{ln(1-\alpha)}{T^2}\right)$ against $1/T$ was linearly regressed. The E_a value was calculated from the slope of the plot, which was divided into parts based on the TGA curves obtained. The thermal degradation of biomasses was reported in detail by Caballero et al. (1997). It initiated at T_i, and the first shoulder peak was attributed to the hemicellulose component. At T_{peak} the rate of cellulose breakdown peaked. Beyond the peak, the thermal decomposition was attributed to lignin. Depending on the amount of hemicellulose in biomass, conversion was ~ 40% of the initial biomass weight, and after the cellulose breakdown, it was ~ 80% of the initial biomass weight.

2.4. Stepwise slow pyrolysis experiments in a batch reactor

After optimizing the mixing ratio and washing duration, a batch reactor was used to perform two-step slow pyrolysis experiments to obtain bio-oil and biochar. The experimental setup has been described in detail in Bhatnagar et al. (2020). The reactor was operated under a continuous nitrogen supply (20 L/ min) for the entire duration of pyrolysis. The sample size for each experiment was 500 g, and a larger particle size of 8–10 mm was used for batch experiments to reduce energy consumed for size reduction. For pyrolysis of the biomass blends, 250 g of each sample was used. The samples were heated from 20 °C to 340 °C in the first step and 340 °C to 600 °C in the second step. The heating rate in both steps was 5 °C/ min. The temperature was maintained at 340 °C for 15 min to collect the bio-oil from the first step, but no isothermal step was required for the second step. The choice of these temperatures was based on the DTG/TGA curves of biomasses. Biochar was collected at the end of the batch run. The gases were not collected in this setup. The yields (y_p, wt%) of the biochar and bio-oil were obtained using Equation (8), and the yield (wt%) of pyrolysis gases was calculated by difference (%Gas = 100 – %bio-oil – %biochar).

$$y_p(\text{wt.}\%) = \left(\frac{w_p * 100}{w_{sample}}\right) \tag{8}$$

Here, w_p is the weight (in grams) of char or bio-oil fractions collected after the reaction and w_{sample} is the initial weight (in grams) of the individual washed/unwashed biomass sample or the optimized biomass blends.

2.5. Biochar and bio-oil characterization

Biochar composition was determined using the methods described in Section 2.1. The pH of char samples was measured in the supernatant of aqueous solution (char to water = 1:10, w/v) using a Metronohm 780 pH Meter. Biochar samples were analyzed using a Jeol JSM-IT500 scanning electron microscope (SEM) equipped with an energy-dispersive X-ray spectrometer (EDS) to characterize the effect of pyrolysis on the biomasses.

The water content of the bio-oil fractions was measured by Karl Fisher titration using Hydranal titrant and Hydranal solvent. The chemical composition was analyzed using gas chromatography with mass spectroscopy (GC/MS), and high-pressure liquid chromatography (HPLC). The detailed analytical procedures are described in Bhatnagar et al. (2021). Each analysis was performed in triplicate, and the standard deviations have been reported. Based on the analysis, 13 chemicals with the highest peak areas were quantified: levoglucosan, acetic acid, furfural, γ-butyrolactone, 2-(5H)-furanone, 2-hydroxy-3-methyl-2-cyclopenten-1-one (cyclotene), phenol, 2-methoxy phenol (guaiacol), 4-methyl-2-methoxy phenol (p-methyl guaiacol), 1,2-dihydroxybenzene (catechol), 4-ethyl-2-methoxy phenol (p-ethyl guaiacol), 4-hydroxy-3-methoxybenzaldehyde (vanillin), and 4-propenyl-2-methoxy phenol

Table 1
Composition of biomass and biomass blends with a standard deviation.

Blending ratio	RS	RS–GNS (1:1)	RS–GNS (1:2)	RS–GNS (1:3)	GNS	RS–WS (1:1)	RS–WS (1:2)	RS–WS (1:3)	WS
%Moisture (ar*)	6.6 ± 0.4	6.3 ± 0.4	6.0 ± 0.3	6.1 ± 0.3	5.4 ± 0.3	5.3 ± 0.3	4.0 ± 0.3	4.6 ± 0.3	4.6 ± 0.2
%Ash (ar*)	16.0 ± 0.5	9.9 ± 0.4	8.2 ± 0.4	6.2 ± 0.4	2.6 ± 0.4	12.8 ± 0.6	11.3 ± 0.6	9.1 ± 0.9	7.7 ± 0.6
%Volatile (ar*)	62.1 ± 0.9	66.3 ± 1.9	68.7 ± 0.2	67.4 ± 2.4	62.1 ± 2.9	65.7 ± 1.0	67.2 ± 1.1	65.7 ± 0.3	67.9 ± 0.1
%Fixed Carbon[a] (ar*)	16.2 ± 0.6	17.5 ± 0.5	17.2 ± 0.5	20.3 ± 0.5	23.8 ± 0.4	16.2 ± 0.4	17.5 ± 0.4	20.6 ± 0.5	20.2 ± 0.3
% C (dry)	37.7 ± 0.1	43.2 ± 0.1	45.0 ± 0.1	45.9 ± 0.1	48.6 ± 0.1	40.4 ± 0.1	41.9 ± 0.1	42.7 ± 0.2	44.3 ± 0.1
% H (dry)	6.5 ± 0.2	6.7 ± 0.3	6.7 ± 0.3	6.7 ± 0.3	6.8 ± 0.3	6.0 ± 0.2	6.3 ± 0.1	6.0 ± 0.7	5.8 ± 0.1
% N (dry)	0.7 ± 0.0	0.8 ± 0.0	0.8 ± 0.0	0.9 ± 0.0	0.9 ± 0.0	0.5 ± 0.0	0.5 ± 0.0	0.6 ± 0.8	0.5 ± 0.0
% O[b] (dry)	39.1 ± 0.3	39.5 ± 0.4	39.3 ± 0.4	40.3 ± 0.4	41.0 ± 0.4	40.4 ± 0.2	40.1 ± 0.1	41.7 ± 0.5	40.7 ± 0.1
% Na (dry)	1.5 ± 0.1	0.8 ± 0.01	0.6 ± 0.02	0.5 ± 0.01	0.2 ± 0.01	0.8 ± 0.1	0.6 ± 0.0	0.5 ± 0.8	0.1 ± 0.0
% Mg (dry)	0.2 ± 0.002	0.2 ± 0.05	0.1 ± 0.009	0.1 ± 0.005	0.1 ± 0.002	0.2 ± 0.001	0.1 ± 0.004	0.1 ± 0.2	0.1 ± 0.04
% K (dry)	1.8 ± 0.1	1.4 ± 0.2	1.3 ± 0.2	1.2 ± 0.2	1.0 ± 0.3	1.7 ± 0.1	1.6 ± 0.1	1.6 ± 0.4	1.5 ± 0.1
% Ca (dry)	0.4 ± 0.0	0.4 ± 0.1	0.4 ± 0.1	0.4 ± 0.1	0.4 ± 0.1	0.3 ± 0.1	0.3 ± 0.1	0.3 ± 0.4	0.3 ± 0.1

* as received; [a]%Fixed carbon (ar) = 100- %Volatile (ar)- %Ash (ar)- %Moisture (ar); [b]%O (dry): 100- %C (dry)- %H (dry)- %N (dry)- %O (dry)- %Ash (dry).

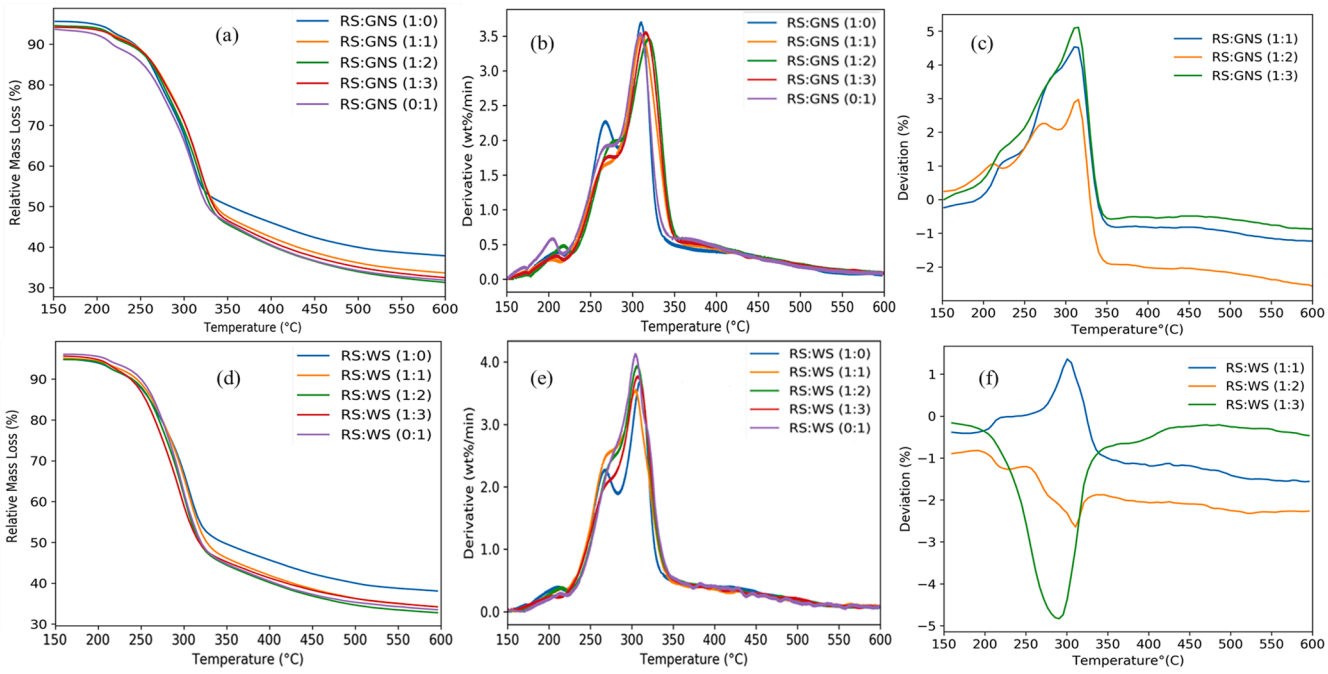

Fig. 1. a) Relative mass loss of RS–GNS blends, b) Derivative mass loss (wt%/min) of RS–GNS blends, c) Deviation % for RS–GNS blends, d) Relative mass loss of RS–WS blends, e) Derivative mass loss (wt%/min) of RS–WS blends, f) Deviation % for RS–WS blends.

(isoeugenol). The concentration of these chemicals has been reported based on dry biomass in Fig. 4. These were obtained by adding the concentration of each chemical in both bio-oil fractions. The composition (mg/kg bio-oil) and water yield (wt% in bio-oil) of individual bio-oil fractions are provided in the supplementary file.

3. Results and discussion

3.1. Determining the effect of biomass blending

Table 1 shows the composition of RS compared to WS and GNS and

Table 2
Parameters of thermal analysis and activation energy (†Synergistic effect (%) from predicted values shown in parenthesis).

Sample	T_i (°C)	T_{peak} (°C)	DTG_{peak} (wt%/min)	D_i† (x10^{-7}, wt%^{2} min^{-2} °C^{-3})	Total volatile yield† (%)	E_a†, α ≤ 0.4 (kJ/mol)	E_a†, α ≤ 0.8 (kJ/mol)
RS unwashed	226.1	310.5	3.7	5.9	62.1	46.4	90.3
RS–GNS (1:1)	224.2	312.2	3.5	6.5(+0.43)	66.3(+1.1)	33.8(-4.9)	87.5(+2.5)
RS–GNS (1:2)	229.5	321.8	3.4	6.5(+0.38)	68.7(+2.5)	35.6(-0.6)	87.6(+4.4)
RS–GNS (1:3)	223.8	318.1	3.5	6.5(+0.35)	67.4(+0.8)	34.2(-0.7)	88.0(+5.7)
GNS unwashed	223.2	312.1	3.5	6.2	68.2	31.1	79.6
RS–WS (1:1)	222.7	306.4	3.7	6.5(-0.03)	65.7(+0.7)	42.7(-5.5)	90.1(-5.5)
RS–WS (1:2)	229.5	305.1	3.9	6.7(-0.09)	67.2(+1.2)	43.7(-5.1)	99.0(+1.7)
RS–WS (1:3)	226.9	306.7	3.5	6.0(-0.87)	65.7(-0.8)	50.4(+1.3)	86.6(-11.5)
WS unwashed	229.4	305.3	4.1	7.2	62.1	50.0	100.8
RS (30 min)	224.4	325.4	3.8	9.3	67.3	68.8	97.9
RS (60 min)	232.0	328.4	4.3	10.3	62.8	72.0	112.1
RS (120 min)	233.6	329.0	4.5	10.8	66.3	79.4	116.4

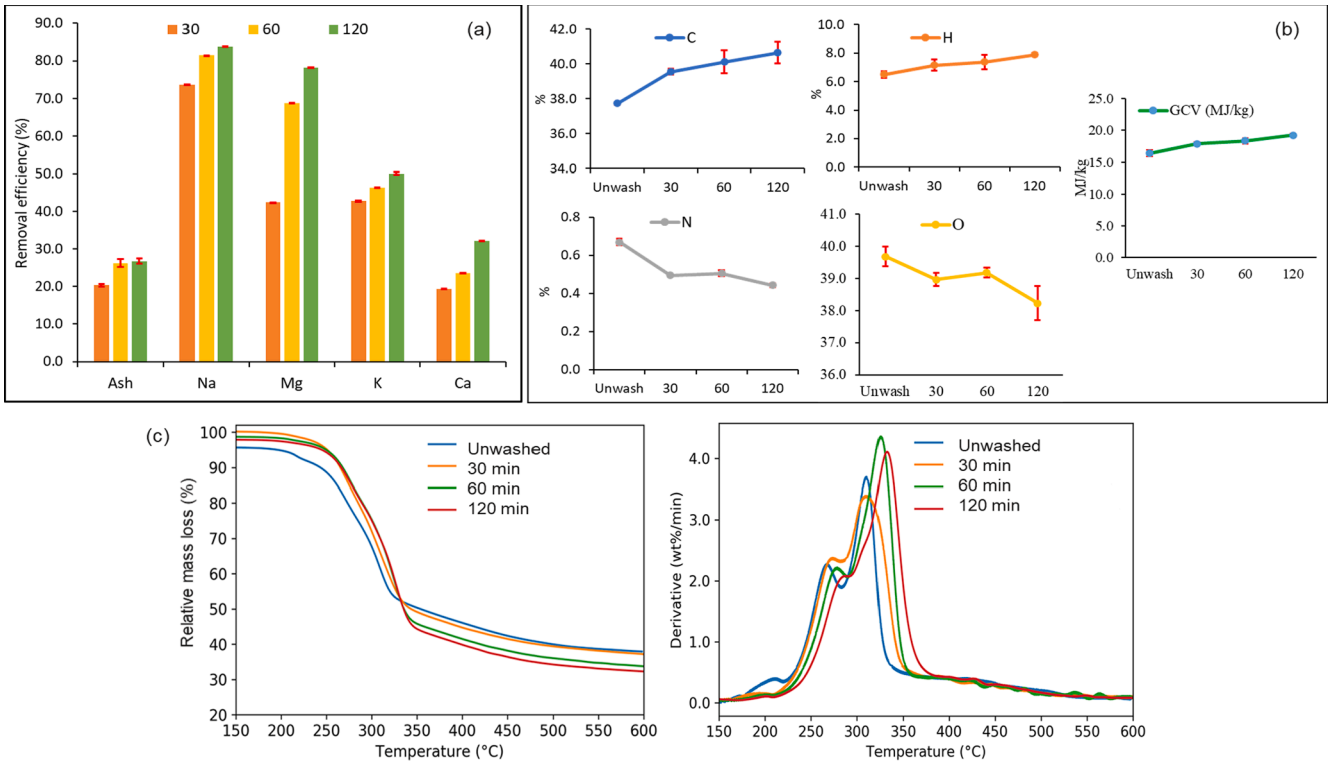

Fig. 2. Effect of washing on a) removal efficiency (%) of ash, b) composition and HHV of RS after washing, c) TGA curves of washed and unwashed RS.

their blends. The ash content of RS was 16.0%, while those of GNS and WS were 2.6% and 7.7%, respectively. Consequently, the ash contents in RS–GNS and RS–WS blends were 6–10% and 2–6% lower than in RS, respectively (absolute difference). A comparison of the distributions of C, H, and O in the blended samples (N < 0.5%) showed that compared to RS, the C content increased by 6–8% (absolute increase) upon adding GNS and by 2.7–5.0% upon adding WS. Conversely, the O content was reduced in both the RS–GNS and RS–WS blends compared to RS.

Moreover, the ash content steadily declined with an increasing amount of GNS or WS. The Na content in the RS–GNS blends were 43–65% lower than in RS, and the K content was 23–35% lower than in RS. As shown in Fig. 1 (TGA/DTG curves) and Table 2, the changes in biomass composition influenced the overall thermal breakdown. Blending RS with GNS and WS increased the total volatile yields (absolute difference) by 3–6% due to the higher volatile contents of GNS and WS compared to RS. Devolatilization also increased through blending, as indicated by the blends' higher D_i values compared to RS.

Fig. 1a–b shows the TGA/DTG curves of RS–GNS blends, and Fig. 1c shows the synergistic effect on their overall thermal degradation. Before reaching 340 °C, the synergistic effect was positive in all co-pyrolysis experiments with GNS blends. In contrast, Fig. 1f shows that in RS–WS, it was positive only for 1:1 blends. Beyond the 1:1 ratio, the ash and lignin contents in these blends may negatively affect the pyrolysis product yield. This was evident in their activation energy (E_a) values (Table 2). The E_a values did not follow a uniform trend with the addition of GNS, although they were between the values observed for RS and GNS separately. However, with an increase in WS in the blends, the E_a values followed the same trend as the volatile yields, and at 1:3, they increased compared to RS. The deviations between the predicted and observed $E_a$values were governed by the same synergistic effect observed in the volatile yields (in Fig. 1).

Based on the TGA/DTG curves and biopolymer distribution in the three biomasses, a mechanism of synergistic effect may be speculated. GNS typically contains 30% lignin, 18% hemicellulose, and 35.7% cellulose. In contrast, RS and WS have 13–16% lignin, and 23–29% hemicellulose, and 31–37% cellulose (Raveendran et al., 1995). The holocellulose (hemicellulose + cellulose) content is in the order of WS > RS > GNS. As mentioned in Section 1, the lignin component degrades over a wide temperature range during pyrolysis, while the holocellulose component breaks down at < 400 °C (Caballero et al., 1997). Hence, the first stage of thermal breakdown depends on the lignin macromolecule and holocellulose cracking. Despite the similar values obtained for T_i (Table 2), GNS broke down faster than RS and at a lower temperature (Fig. 1a) due to the higher lignin content. This cracking of GNS promoted RS breakdown, yielding more volatiles than predicted, which led to a positive value of the synergistic effect below 340 °C (Fig. 1c). This was also observed by Mallick et al. (2018) in the pyrolysis of 1:1 blends (w/w) of sawdust and rice husk. The rapid breakdown of sawdust promoted holocellulose breakdown in rice husk. In turn, the high ash content (19.7%) in rice husk enhanced sawdust cracking. As the temperature increased, lignin became more recalcitrant, and due to the higher holocellulose content in RS–WS blends, a higher DTG_{peak} was observed in RS–WS blends than in RS–GNS blends. Beyond 340 °C, the lignin content and composition came into play. The lignin macromolecule contains syringyl and guaiacyl units connected by ether bonds (Asmadi et al., 2011). Syringyl units crack more easily than guaiacyl units. Since GNS had the highest lignin content and highest volatile yields beyond 340 °C, it is likely that it contained more syringyl units, leading to higher (than predicted) total volatile yields in RS–GNS than RS–WS blends at higher temperatures.

These results were used to optimize the blending ratio for co-pyrolysis. Beyond the 1:2 ratio, the thermal behavior did not show significant improvement. However, the synergistic effect observed during mass loss had the highest positive deviation for 1:1 blends. Hence, 1:1 blends were used for pyrolysis studies in the batch reactor (see Section 3.4).

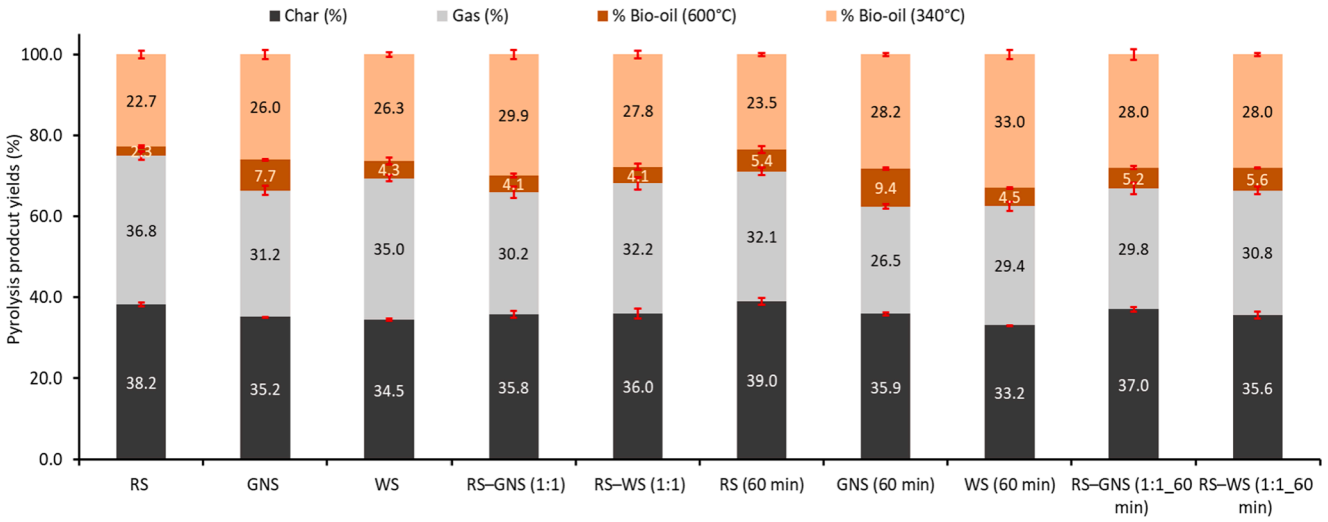

Synergistic effect (%)	RS–GNS (1:1)	RS–WS (1:1)	RS–GNS (1:1_60 min)	RS–WS (1:1_60 min)
% Bio-oil (340°C)	+5.6	+3.3	+2.1	-0.3
% Bio-oil (600°C)	-0.9	+0.8	-2.2	+0.7
% Total Bio-oil	+4.7	+4.0	-0.1	+0.4
% Char	-0.9	-0.3	-0.4	-0.5
% Gas	-3.7	-3.7	+0.5	+0.1

Fig. 3. Yields (%) of pyrolysis products obtained from batch reactor studies.

3.2. *Comparison of the effects of the washing duration on composition*

The subsequent experiments aimed to investigate the effect of washing on RS composition. Fig. 2 and Table 2 and S2 show the results of the washing pretreatment. The washing time played a significant role in removing Na and K from RS. After washing for 120 min, the total ash removal efficiency was 26.8% (Fig. 2a), while the real mass yields ranged from 88.2% to 88.7% (Table S2). The high removal efficiency of ash contents (15–41%) has also been reported in other RS washing studies (Deng et al., 2013; Yu et al., 2014). The mass yields indicated that during washing, some organic components of RS leached out. Previous washing studies have shown that this is inevitable in washing pretreatment due to the removal of water-soluble compounds, such as organic acids (acetic acid, formic acid, and lactic acid), sugars (arabinose, glucose, mannose, and xylose), waxes, and phthalic acid esters (Long et al., 2020; Yu et al., 2014).

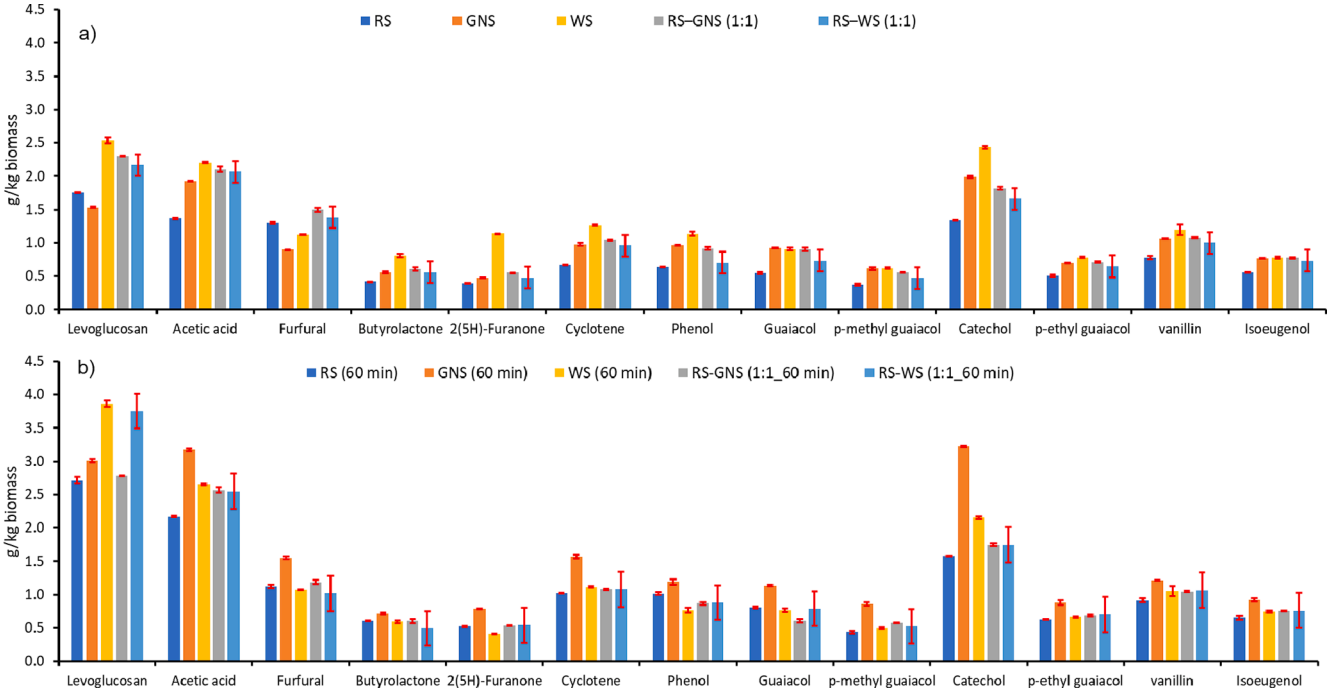

Fig. 4. Bio-oil compositions obtained from (a) unwashed samples, (b) washed samples with standard deviations from three replicates.

After washing, the AAEM removal efficiency was in the order of Na (73.6–83.8%) > Mg (42.4–78.2%) > K (42.7–50.1%) > Ca (19.4–32.2%). Most Na and K were removed within 30 min because these alkali metals exist as water-soluble compounds in the crop residues, such as NaCl, KCl, K_2SO_4, KNO_3, $NaNO_3$, Na_2SO_4, and K_3PO_4 (Niu et al., 2016; Vassilev et al., 2012). The Na and K removal efficiency plateaued after 60 min. Conversely, the alkali earth metals (Ca and Mg) showed continuous removal (up to 9%) upon prolonging the washing time from 60 to 120 min. The organic compounds in the leachate facilitated this additional removal. Since Ca and Mg constitute a considerable part of the biomass structure and are more strongly bound to the organic matrix than K and Na, they do not leach out with water alone (Hawkesford et al., 2012). However, the organic acids and sugar present in the leachate facilitated the leaching of Ca and Mg compounds. This was most prominent with longer washing durations (>30 min) and has also been observed in the washing of wheat straw (Singhal et al., 2021). Apart from removing ash and AAEMs, increasing the washing duration led to a continuous increase in C and H contents and reduced N-content (Fig. 2b). The N content reduction resulted from removing water-soluble ions, such as NH_4^+ and NO_3^- from RS (Vassilev et al., 2012). Due to this change in composition, the GCV values increased by 2.9 MJ/kg—that is, by 17.5%— after 120 min of washing compared to unwashed RS.

The TGA curves in Fig. 2c also show that washing improved the resolution of peaks at 260–280 °C, indicating a higher hemicellulose breakdown, and at 310–330 °C, indicating a higher cellulose breakdown. As the washing duration increased, the total volatile yields increased by up to 5% (Table 2), with a corresponding improvement in the D_i values. However, an increase in the washing duration led to a rise in the E_a values. This may have been caused by reducing the water-soluble structures due to pretreatment and ash, such as Na and K, which promote biomass cracking (Wang et al., 2021; Zhang et al., 2017).

Since mass loss and removal efficiency improvement beyond 60 min of washing were marginal, the batch reactor pyrolysis study was conducted using samples washed for 60 min. As mentioned in Section 2.2, GNS and WS were washed for 60 min and blended in a 1:1 ratio (w/w) with RS to study the combined effects of washing and co-pyrolysis. The compositions of washed GNS and WS are shown in Table S2.

3.3. Pyrolysis product yields

Next, the effects of blending and washing were compared in bio-oil and biochar yields using two-step pyrolysis in a batch reactor. Fig. 3 shows the product yields and synergistic effect values for biomass blends.

Unwashed RS produced the lowest total bio-oil (25%) and highest biochar (38.2%) yields. After blending, the total bio-oil yields increased to 34.0% for RS–GNS (1:1) and 31.9% for RS–WS (1:1). The difference between unwashed blends' predicted and observed bio-oil yields was nearly 4% (Fig. 3). These results were consistent with the increased volatile yields observed in the TGA/DTG curves (Section 3.1). Furthermore, the bio-oil yield at < 340 °C was 5–7% higher in the blends than in RS and only 2% higher at < 600 °C owing to a higher holocellulose breakdown in the first step. Moreover, co-pyrolysis resulted in reduced gas yields for both unwashed blends. The observed gas yields were lower than predicted values due to the synergistic effect of GNS on RS and the reduced AAEM content after blending, which inhibited bio-oil cracking to form gases (as mentioned in Section 3.1). However, the observed char yields were comparable to the predicted yields due to multiple counteractive char-forming reactions. Below 300 °C, char formation is linked with the aromatization of xylan—a building block of hemicellulose (Le Brech et al., 2016). Above 350 °C, the thermal cracking of lignin generates radicals that create aromatic macromolecules, leading to "retrogressive char formation" (Toor et al., 2018).

Improvements were seen in the bio-oil yields of washed biomasses and their blends compared to unwashed RS. The bio-oil yields of RS, GNS, and WS washed for 60 min increased by 4–7% compared to the unwashed RS, GNS, and WS. For all washed samples, the gas yields were lower than for unwashed samples. Moreover, the char amounts in washed and unwashed samples were nearly equal in all cases. However, the difference between the predicted and observed bio-oil yields for washed blends was < 1%, indicating that the AAEM leaching altered the synergistic effect of GNS/WS on RS after leaching.

In line with these observations, Wigley et al. (2016) and Mourant et al. (2011) reported that bio-oil yields from water-washed biomasses improved marginally (up to 4%), with a corresponding reduction in gas yields. This may be explained by comparing the roles of water-soluble and acid-soluble ions in the biomass. Since the acid-soluble ions, such as Ca, are present as carboxylates in the biomass matrix, the removal efficiency through water washing is limited. Hence, they form a chemical bridge between cellulose, hemicellulose, and lignin, preventing depolymerization at higher temperatures (Mourant et al., 2011). Therefore, bio-oil and biochar yields cannot be the only indicators of pyrolysis performance. A detailed evaluation of the quality of the pyrolysis products is presented in Sections 3.4 and 3.5.

3.4. Bio-oil characterization

The bio-oil compositions are shown in Fig. 4. Table S3 shows the chemical yields in individual bio-oil fractions obtained from the two-step pyrolysis studies. The differences between predicted and observed yields due to the synergistic effect are shown in Table S4.

The bio-oil fractions obtained had high water contents due to the slow heating rate used in this study, which increased the vapor residence and promoted condensation reactions in bio-oil vapors (Czernik et al., 1994). As shown in Table S3, biomass blending did not reduce the water content; conversely, washing reduced it from 57% in unwashed RS to 48% in RS washed for 60 min. Similarly, the water content in bio-oil from washed blends was 8–9% lower than that from unwashed blends.

Comparing the chemical yields from bio-oil (in grams per kilogram of biomass) showed that the unwashed RS samples produced lower total yields for almost all quantified chemicals than the RS–GNS and RS–WS blends (Fig. 4). Specifically, RS–GNS (1:1) blend yielded more levoglucosan than both RS and RS–WS (1:1). However, the phenolic yields were lower for the RS–GNS blend than for the unwashed GNS. This was due to the higher lignin content of GNS (Raveendran et al., 1995), which was depolymerized to yield more catechol in pure GNS-derived bio-oil than the blend.

Conversely, all chemical yields (except furfural) were lower in the RS–WS (1:1) blend when compared with pure WS. Furfural is generated from hemicellulose breakdown (see Section 1) in the first step of pyrolysis. However, at higher temperatures, it may be a by-product of the dehydration of levoglucosan due to the catalytic effects of AAEMs. Hence, the difference in furfural content may have been due to the higher K content of the RS–WS blend (1.7%) compared to WS (1.5%) and the lower K content of the RS–GNS (1:1) blend (1.4%) compared to GNS (1%). K increases furans in the bio-oil by converting anhydrosugars to linear aldehydes, furfural, and 5-hydroxymethyl furfural (Zhang et al., 2017).

A further comparison between the furfural yields of WS and RS–WS (1:1) showed that the higher furfural yields were not proportional to the lower levoglucosan yields. The higher furfural yields may have caused hemicellulose breakdown (Peng et al., 2012) in the RS–WS (1:1) blend. As shown in Table S4, the observed levoglucosan yields for RS–GNS were higher than predicted, which may have been due to a reduced ash content after blending.

Fig. 4b shows that levoglucosan yields improved in RS, GNS, and WS washed for 60 min compared to the unwashed biomasses. While all other quantified chemicals also increased in RS and GNS washed for 60 min, the observed yields were lower for all chemicals except levoglucosan and acetic acid in WS (60 min). The yields improved because the Na and K contents decreased, which promoted levoglucosan formation

Table 3
Biochar composition from pyrolysis studies in a batch reactor with a standard deviation.

Biochar from->	RS	GNS	WS	RS–GNS (1:1)	RS–WS (1:1)	RS (60 min)	GNS (60 min)	WS (60 min)	RS–GNS (1:1_60 min)	RS–WS (1:1_60 min)
%Ash	37.1 ± 0.7	8.5 ± 0.1	23.2 ± 0.2	24.4 ± 0.2	32.7 ± 1.0	29.7 ± 0.5	7.1 ± 0.1	20.0 ± 0.01	22.1 ± 0.9	28.7 ± 0.1
pH	10.5 ± 0.01	10.0 ± 0.01	10.8 ± 0.03	10.1 ± 0.01	10.3 ± 0.02	10.3 ± 0.01	9.4 ± 0.04	9.8 ± 0.01	10.2 ± 0.01	10.1 ± 0.02
GCV[a] (MJ/kg)	18.3 ± 0.5	29.4 ± 0.7	23.6 ± 0.2	23.1 ± 0.4	20.9 ± 1.7	20.1 ± 1.1	30.9 ± 0.6	23.5 ± 0.2	23.3 ± 0.02	22.7 ± 0.1
Molar H/C[b]	0.2	0.3	0.3	0.3	0.3	0.3	0.3	0.4	0.2	0.3
Molar O/C[c]	0.1	0.1	0.1	0.1	0.1	0.1	0.04	0.1	0.1	0.1
log $k_{f,\ NAP}$[d]	4.8	4.5	4.9	4.6	4.6	4.7	4.5	4.5	4.7	4.5
N_{NAP}[d]	0.3	0.3	0.2	0.3	0.3	0.3	0.3	0.3	0.3	0.3
log $k_{f,\ PHE}$[d]	4.8	4.6	4.8	4.6	4.7	4.7	4.6	4.6	4.7	4.6
N_{PHE}[d]	0.4	0.4	0.4	0.5	0.5	0.4	0.4	0.5	0.4	0.5
F_u[d]	6.9	5.4	10.4	8.2	7.5	1.9	2.8	5.7	2.4	3.2
S_r[d]	94.1	86.7	92.8	91.2	94.1	95.7	86.9	92.6	93.1	94.2

[a]GCV (MJ/kg) = 0.3491 × C + 1.1783 × H + 0.1005 × S- 0.1034 × O- 0.0151 × N- 0.0211 × Ash; [b]Molar $H/C = \frac{\%H/1.008}{\%C/12.011}$; [c]Molar $O/C = \frac{\%O/15.999}{\%C/12.011}$; [d]Equations provided in supplementary file Table S6.

from cellulose. Furthermore, an increase in acetic acid yields was observed after washing. As reported by Wigley et al. (2016), acetic acid is not produced during the pyrolysis of cellulose. It can only be obtained as a by-product of hemicellulose breakdown—from the cleavage of the acetyl content in hemicellulose—or as a product of polymerization reactions between anhydrosugars and lignin-derived phenolic products in the bio-oil. Hence, the increased yields of levoglucosan and phenolic products may have increased acetic acid yields in the washed samples.

Finally, an evaluation of the integrated effects of washing and blending on two-step pyrolysis revealed that the levoglucosan yield in the RS–GNS (1:1) blend prepared from 60 min washed samples was 1.5 times higher than in unwashed RS–GNS (1:1) blend. Moreover, levoglucosan yields were 2.2 times higher in the RS–WS (1:1) blend prepared from 60 min washed samples than in RS–WS (1:1) blend. This indicated that the integrated effects of co-pyrolysis and washing were more substantial on RS–WS. Interestingly, the phenolic derivatives in washed and unwashed blends were nearly identical, possibly because the lignin component was unaffected by water-washing (Wang et al., 2021).

These results suggest that both GNS and WS may be blended with RS to improve bio-oil quality. Moreover, while GNS may be mixed with unwashed RS, the integrated co-pyrolysis of washed RS–WS blends improves.

3.5. Biochar characterization

The obtained biochar samples obtained in this study were characterized using proximate and ultimate analyses (Table 3 and S5). Comparing the biochar sample compositions showed that the biomass ash content was very high since > 95% of the biomass ash is likely to be retained in the biochar (Leijenhorst et al., 2016). The GCV (in megajoules per kilogram) of char derived from GNS and WS was higher than RS. Consequently, chars of blended biomass also had a higher GCV than RS-derived char, even without washing. However, the biochar application depended on the ash composition (Table S5) and behavior (Table 3). The main ash-forming elements in biochar (in percentage by weight) were Si (5–20%), K (1–5%), and Ca (0.4–1.5%). Si was present as silica (SiO_2) or as various silicate minerals (Zevenhoven et al., 2012). During combustion, the multiple metals connected to silicate usually remain in the silicate matrix and primarily produce high-melting ash. However, in straw, the K and Si contents react to form low-melting products (Zevenhoven et al., 2012). The fouling index (F_u) and the slagging ratio (S_r) are commonly used for assessing coal quality. Zevenhoven et al. (2012) used them as proxies to evaluate the efficacy of biochar as fuel. These indices depend on the ratio of basic compounds (formed by AAEMs) to acidic compounds (formed by Si, Al, Ti). The value of $F_u \leq 0.6$ represents a low fouling risk, while between 0.6 and 40 represent medium to high fouling risks. Biochar obtained from unwashed samples did not fare well in this category. Conversely, washing reduced the risk of fouling to a great extent, with the lowest fouling propensity observed in biochar from 60 min washed RS. The S_r value corresponds to the viscosity of ash, with values of > 72 indicating a low slagging propensity and values of ≤ 65 indicating a high slagging propensity. All biochar samples obtained in this study had a S_r of > 72, indicating their suitability for boiler applications. It is vital to explore the application of biochar as a renewable fuel to improve the environmental and economic performance of decentralized pyrolysis units (Yang et al., 2020).

Multiple reviews have found that biochar may also improve crop productivity when added to the soil since it can alter the bioavailability of soil contaminants, prevent NOx and CH_4 emissions, and correct the soil pH (Ghodake et al., 2021; Ronsse et al., 2013; Spokas, 2010; Xiao et al., 2016). The molar ratios of H/C and O/C and AAEM-content have been used as proxies to assess biochar's adsorption capacity and its effect on and stability in the soil (Ronsse et al., 2013). These values determine the aromaticity of biochar and are a function of the initial biomass composition, pyrolysis temperature, volatile content, and pre-or post-production treatment. Xiao et al. (2016) correlated the H/C molar ratio and the Freundlich fitting parameters of adsorption to determine the fate of model soil contaminants naphthalene (NAP) and phenanthrene (PHE). For NAP and PHE, the parameter *N* generally increased as log K_f decreased with an increasing H/C molar ratio (Fig. S1). This indicates that higher aromaticity may allow better immobilization of soil contaminants. Spokas (2010) reported that biochar products with O/C ratios of < 0.2 have an overall half-life of ≥ 1000 years, whereas, for O/C ratios of ≥ 0.6, the predicted half-life drops to < 100 years. The molar ratio of O/C is also directly linked to the cation exchange capacity of biochar samples, which is related to the innate negative charge on the oxygen-based functional groups that can collect cations (Ghodake et al., 2021). Although a higher O/C ratio increases the CEC, it may also lead to a short life of biochar in the soil. The pH of biochar depends on its ash content and the presence of oxygen functionalities in it. At a pyrolysis temperature of > 600 °C, the carboxyl groups in the resulting biochar are likely to be reduced, or the acidic groups become deprotonated to the conjugate bases, resulting in a more alkaline biochar (Ronsse et al., 2013). These can be applied to acidic soils and, over time, restore the soil pH for microbial activity.

All char samples showed nearly equal potential for NAP and PHE adsorption. The results are comparable to those reported by Xiao et al. (2016) for other biomasses, such as orange peels, pinewood, and rice straw, produced at or above 600 °C through slow pyrolysis. The O/C values were < 0.2 and were comparable to those of other biochar samples (0.008–0.72) evaluated by Schaffer et al. (2019) for laboratory-based pyrolysis systems. Moreover, the pH values of all char samples were 9–10, indicating high alkalinity. These parameters suggest that all

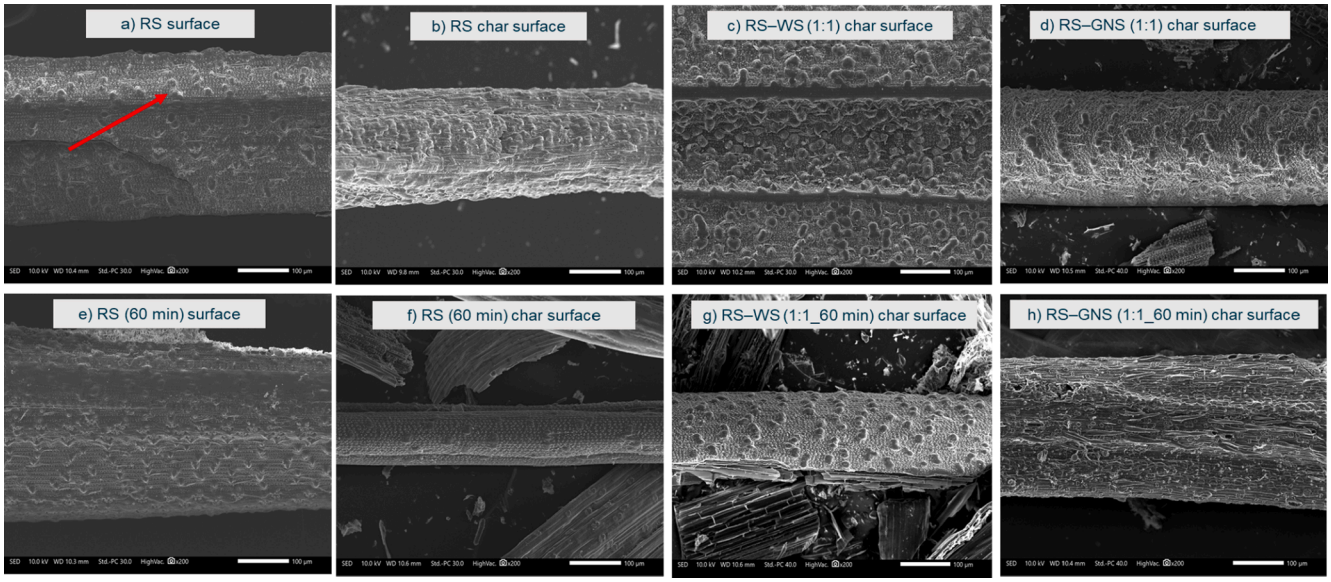

Fig. 5. SEM images (scale bar: 100 μm) of unwashed and washed RS and biochar derived from unwashed and washed blends. The arrows indicate the typical features in the cross-sections.

RS-derived chars were potentially suitable for soil amendment, particularly in acidic soils, with a likely half-life of > 1000 years. However, long-term experiments are required to confirm these findings, and such experiments were beyond the scope of this study.

The changes in the surface morphology of rice straw after pretreatment and co-pyrolysis were observed using SEM (Fig. 5 and S2). A key observation was the presence of several nodes on the surface of RS with a bubble-like appearance (shown in Fig. 5a). The EDS point analyses indicated that these nodes had a high silica concentration. After washing and co-pyrolysis, fewer nodes were observed on the char surface due to lower silica content in the biochar sample (Table S5). However, the structures were broadly similar, confirming that water washing does not alter the sample's biopolymer composition (Mourant et al., 2011).

The results in this study point to various applications of bio-oil and biochar products from slow two-step pyrolysis of rice straw if the ash content is reduced via pretreatment or co-pyrolysis. Furthermore, the findings show that the co-pyrolysis of washed blends improves bio-oil quality and is beneficial for the obtained biochar.

4. Conclusions

This comprehensive study evaluated the combined effects of water washing and blending on the two-step pyrolysis of rice straw. The results showed that the catalytic effects of AAEMs were inhibited by blending low- and high-ash biomasses or by leaching out water-soluble elements from biomass. This increased the bio-oil yield and decreased the gas yields during pyrolysis. Furthermore, two-step pyrolysis generated levoglucosan-rich and phenolic-rich bio-oil fractions. The obtained biochar had lower fouling and slagging propensities than rice straw and a higher GCV. This suggests that it could be used in boilers as fuel. Moreover, it has potential applications in soil for contaminant adsorption, depending on the composition. Overall, the findings suggest that the pyrolysis of pretreated rice straw and locally available crop residues could generate multiple value-added products.

Declaration of Competing Interest

The authors declare that they have no known competing financial interests or personal relationships that could have appeared to influence the work reported in this paper.

Acknowledgement

This work made use of Tampere Microscopy Center facilities at Tampere University. The authors also acknowledge the help of Mr Sujai Banerji in data analysis and interpretation.

Appendix A. Supplementary material

Supplementary data to this article can be found online at https://doi.org/10.1016/j.wasman.2021.12.013.

References

Abnisa, F., Wan Daud, W.M.A., 2014. A review on co-pyrolysis of biomass: An optional technique to obtain a high-grade pyrolysis oil. Energy Convers. Manag. 87, 71–85. https://doi.org/10.1016/j.enconman.2014.07.007.

Alvarez, J., Amutio, M., Lopez, G., Santamaria, L., Bilbao, J., Olazar, M., 2019. Improving bio-oil properties through the fast co-pyrolysis of lignocellulosic biomass and waste tyres. Waste Manag. 85, 385–395. https://doi.org/10.1016/j.wasman.2019.01.003.

Bandara, Y.W., Gamage, P., Gunarathne, D.S., 2020. Hot water washing of rice husk for ash removal: The effect of washing temperature, washing time and particle size. Renew. Energy 153, 646–652. https://doi.org/10.1016/J.RENENE.2020.02.038.

Bhatnagar, A., Barthen, R., Tolvanen, H., Konttinen, J., 2021. Bio-oil stability through stepwise pyrolysis of groundnut shells: Role of chemical composition, alkali and alkaline earth metals, and storage conditions. J. Anal. Appl. Pyrolysis 157, 105219. https://doi.org/10.1016/j.jaap.2021.105219.

Bhatnagar, A., Tolvanen, H., Konttinen, J., 2020. Potential of stepwise pyrolysis for on-site treatment of agro-residues and enrichment of value-added chemicals. Waste Manag. 118, 667–676. https://doi.org/10.1016/j.wasman.2020.09.022.

Caballero, J.A., Conesa, J.A., Font, R., Marcilla, A., 1997. Pyrolysis kinetics of almond shells and olive stones considering their organic fractions. J. Anal. Appl. Pyrolysis 42, 159–175. https://doi.org/10.1016/S0165-2370(97)00015-6.

Cai, J., Bi, L., 2008. Precision of the Coats and Redfern Method for the Determination of the Activation Energy without Neglecting the Low-Temperature End of the Temperature Integral. Energy Fuels 22, 2172–2174. https://doi.org/10.1021/ef8002125.

Cao, B., Wang, S., Hu, Y., Abomohra, A.E.F., Qian, L., He, Z., Wang, Q., Uzoejinwa, B.B., Esakkimuthu, S., 2019. Effect of washing with diluted acids on Enteromorpha clathrata pyrolysis products: Towards enhanced bio-oil from seaweeds. Renew. Energy 138, 29–38. https://doi.org/10.1016/J.RENENE.2019.01.084.

Channiwala, S.A., Parikh, P.P., 2002. A unified correlation for estimating HHV of solid, liquid and gaseous fuels. Fuel. https://doi.org/10.1016/S0016-2361(01)00131-4.
Chen, D., Wang, Y., Liu, Y., Cen, K., Cao, X., Ma, Z., Li, Y., 2019. Comparative study on the pyrolysis behaviors of rice straw under different washing pretreatments of water, acid solution, and aqueous phase bio-oil by using TG-FTIR and Py-GC/MS. Fuel 252, 1–9. https://doi.org/10.1016/J.FUEL.2019.04.086.
Chen, W., Chen, Y., Yang, H., Xia, M., Li, K., Chen, X., Chen, H., 2017. Co-pyrolysis of lignocellulosic biomass and microalgae: Products characteristics and interaction effect. Bioresour. Technol. 245, 860–868. https://doi.org/10.1016/j.biortech.2017.09.022.
Czernik, S., Johnson, D.K., Black, S., 1994. Stability of wood fast pyrolysis oil. Biomass Bioenergy 7, 187–192. https://doi.org/10.1016/0961-9534(94)00058-2.
de Wild, P.J., den Uil, H., Reith, J.H., Kiel, J.H.A., Heeres, H.J., 2009. Biomass valorisation by staged degasification: A new pyrolysis-based thermochemical conversion option to produce value-added chemicals from lignocellulosic biomass. J. Anal. Appl. Pyrolysis 85, 124–133. https://doi.org/10.1016/J.JAAP.2008.08.008.
Deng, L., Zhang, T., Che, D., 2013. Effect of water washing on fuel properties, pyrolysis and combustion characteristics, and ash fusibility of biomass. Fuel Process. Technol. 106, 712–720. https://doi.org/10.1016/j.fuproc.2012.10.006.
Devi, S., Gupta, C., Jat, S.L., Parmar, M.S., 2017. Crop residue recycling for economic and environmental sustainability: The case of India. Open Agric. 2, 486–494.
Directorate of Economics & Statistics, 2020. Agricultural statistics at a glance 2019.
Eom, I.Y., Kim, J.Y., Lee, S.M., Cho, T.S., Yeo, H., Choi, J.W., 2013. Comparison of pyrolytic products produced from inorganic-rich and demineralized rice straw (Oryza sativa L.) by fluidized bed pyrolyzer for future biorefinery approach. Bioresour. Technol. 128, 664–672. https://doi.org/10.1016/j.biortech.2012.09.082.
FAO, 2021. Crops and livestock products [WWW Document]. URL https://www.fao.org/faostat/en/#data/QCL (accessed 10.17.21).
Fytili, D., Zabaniotou, A., 2018. Circular Economy Synergistic Opportunities of Decentralized Thermochemical Systems for Bioenergy and Biochar Production Fueled with Agro-industrial Wastes with Environmental Sustainability and Social Acceptance: a Review. Curr. Sustain. Energy Reports 5, 150–155. https://doi.org/10.1007/s40518-018-0109-5.
Ghodake, G.S., Shinde, S.K., Kadam, A.A., Saratale, R.G., Saratale, G.D., Kumar, M., Palem, R.R., AL-Shwaiman, H.A., Elgorban, A.M., Syed, A., Kim, D.-Y., 2021. Review on biomass feedstocks, pyrolysis mechanism and physicochemical properties of biochar: state-of-the-art framework to speed up vision of circular bioeconomy. J. Clean. Prod. 126645. 10.1016/j.jclepro.2021.126645.
Hawkesford, M., Horst, W., Kichey, T., Lambers, H., Schjoerring, J., Møller, I.S., White, P., 2012. Functions of Macronutrients, in: Marschner's Mineral Nutrition of Higher Plants. Elsevier, pp. 135–189. 10.1016/B978-0-12-384905-2.00006-6.
He, Q., Guo, Q., Ding, L., Gong, Y., Wei, J., Yu, G., 2018. Co-pyrolysis Behavior and Char Structure Evolution of Raw/Torrefied Rice Straw and Coal Blends. Energy Fuels 32, 12469–12476. https://doi.org/10.1021/acs.energyfuels.8b03469.
Huang, Y., Liu, S., Akhtar, M.A., Li, B., Zhou, J., Zhang, S., Zhang, H., 2020. Volatile–char interactions during biomass pyrolysis: Understanding the potential origin of char activity. Bioresour. Technol. 316, 123938 https://doi.org/10.1016/j.biortech.2020.123938.
Klinar, D., 2016. Universal model of slow pyrolysis technology producing biochar and heat from standard biomass needed for the techno-economic assessment. Bioresour. Technol. 206, 112–120. https://doi.org/10.1016/j.biortech.2016.01.053.
Le Brech, Y., Raya, J., Delmotte, L., Brosse, N., Gadiou, R., Dufour, A., 2016. Characterization of biomass char formation investigated by advanced solid state NMR. Carbon N. Y. 108, 165–177. https://doi.org/10.1016/J.CARBON.2016.06.033.
Leijenhorst, E.J., Wolters, W., van de Beld, L., Prins, W., 2016. Inorganic element transfer from biomass to fast pyrolysis oil: Review and experiments. Fuel Process. Technol. 149, 96–111. https://doi.org/10.1016/j.fuproc.2016.03.026.
Li, S., Wang, C., Luo, Z., Zhu, X., 2020. Investigation on the Catalytic Behavior of Alkali Metals and Alkaline Earth Metals on the Biomass Pyrolysis Assisted with Real-Time Monitoring. Energy Fuels 34, 12654–12664. https://doi.org/10.1021/acs.energyfuels.0c01938.
Long, J., Deng, L., Che, D., 2020. Analysis on organic compounds in water leachate from biomass. Renew. Energy 155, 1070–1078. https://doi.org/10.1016/j.renene.2020.04.033.
Mante, O.D., Dayton, D.C., Soukri, M., 2016. Production and distillative recovery of valuable lignin-derived products from biocrude. RSC Adv. 6, 94247–94255. https://doi.org/10.1039/C6RA21134H.
Mohan, D., Pittman, Charles U., Steele, P.H., 2006. Pyrolysis of Wood/Biomass for Bio-oil: A Critical Review. Energy & Fuels 20, 848–889. https://doi.org/10.1021/ef0502397.
Mourant, D., Wang, Z., He, M., Wang, X.S., Garcia-Perez, M., Ling, K., Li, C.Z., 2011. Mallee wood fast pyrolysis: Effects of alkali and alkaline earth metallic species on the yield and composition of bio-oil. Fuel 90, 2915–2922. https://doi.org/10.1016/j.fuel.2011.04.033.
Niu, Y., Tan, H., Hui, S., 2016. Ash-related issues during biomass combustion: Alkali-induced slagging, silicate melt-induced slagging (ash fusion), agglomeration, corrosion, ash utilization, and related countermeasures. Prog. Energy Combust. Sci. 52, 1–61. https://doi.org/10.1016/j.pecs.2015.09.003.
Özsin, G., Pütün, A.E., 2018. A comparative study on co-pyrolysis of lignocellulosic biomass with polyethylene terephthalate, polystyrene, and polyvinyl chloride: Synergistic effects and product characteristics. J. Clean. Prod. 205, 1127–1138. https://doi.org/10.1016/j.jclepro.2018.09.134.
Peng, F., Peng, P., Xu, F., Sun, R.-C., 2012. Fractional purification and bioconversion of hemicelluloses. Biotechnol. Adv. 30, 879–903. https://doi.org/10.1016/J.BIOTECHADV.2012.01.018.
Raveendran, K., Ganesh, A., Khilar, K.C., 1995. Influence of mineral matter on biomass pyrolysis characteristics. Fuel 74, 1812–1822. https://doi.org/10.1016/0016-2361(95)80013-8.
Ronsse, F., van Hecke, S., Dickinson, D., Prins, W., 2013. Production and characterization of slow pyrolysis biochar: influence of feedstock type and pyrolysis conditions. GCB Bioenergy 5, 104–115. https://doi.org/10.1111/gcbb.12018.
Schaffer, S., Pröll, T., Al Afif, R., Pfeifer, C., 2019. A mass- and energy balance-based process modelling study for the pyrolysis of cotton stalks with char utilization for sustainable soil enhancement and carbon storage. Biomass Bioenergy 120, 281–290. https://doi.org/10.1016/j.biombioe.2018.11.019.
Singh, G., Gupta, M.K., Chaurasiya, S., Sharma, V.S., Pimenov, D.Y., 2021. Rice straw burning: a review on its global prevalence and the sustainable alternatives for its effective mitigation. Environ. Sci. Pollut. Res. https://doi.org/10.1007/s11356-021-14163-3.
Singhal, A., Konttinen, J., Joronen, T., 2021. Effect of different washing parameters on the fuel properties and elemental composition of wheat straw in water-washing pre-treatment. Part 1: Effect of washing duration and biomass size. Fuel 292, 120206. https://doi.org/10.1016/j.fuel.2021.120206.
Spokas, K.A., 2010. Review of the stability of biochar in soils: predictability of O: C molar ratios. Carbon Manag. 1, 289–303. https://doi.org/10.4155/cmt.10.32.
Toor, S.S., Rosendahl, L., Sintamarean, I., 2018. Recipe-based co-HTL of biomass and organic waste. Direct Thermochem. Liq. Energy Appl. 169–189 https://doi.org/10.1016/B978-0-08-101029-7.00005-9.
Vassilev, S.V., Baxter, D., Andersen, L.K., Vassileva, C.G., Morgan, T.J., 2012. An overview of the organic and inorganic phase composition of biomass. Fuel 94, 1–33. https://doi.org/10.1016/j.fuel.2011.09.030.
Wang, S., Dai, G., Yang, H., Luo, Z., 2017. Lignocellulosic biomass pyrolysis mechanism: A state-of-the-art review. Prog. Energy Combust. Sci. 62, 33–86. https://doi.org/10.1016/J.PECS.2017.05.004.
Wang, Z., Wang, Q., Yang, X., Xia, S., Zheng, A., Zeng, K., Zhao, Z., Li, H., Sobek, S., Werle, S., 2021. Comparative Assessment of Pretreatment Options for Biomass Pyrolysis: Linking Biomass Compositions to Resulting Pyrolysis Behaviors, Kinetics, and Product Yields. Energy Fuels 35, 3186–3196. https://doi.org/10.1021/acs.energyfuels.0c04186.
Wigley, T., Yip, A.C.K., Pang, S., 2016. Pretreating biomass via demineralisation and torrefaction to improve the quality of crude pyrolysis oil. Energy 109, 481–494. https://doi.org/10.1016/j.energy.2016.04.096.
Xiao, X., Chen, Z., Chen, B., 2016. H/C atomic ratio as a smart linkage between pyrolytic temperatures, aromatic clusters and sorption properties of biochars derived from diverse precursory materials. Sci. Rep. 6, 22644. https://doi.org/10.1038/srep22644.
Yang, X., Han, D., Zhao, Y., Li, R., Wu, Y., 2020. Environmental evaluation of a distributed-centralized biomass pyrolysis system: A case study in Shandong. China. Sci. Total Environ. 716, 136915 https://doi.org/10.1016/J.SCITOTENV.2020.136915.
Yu, C., Thy, P., Wang, L., Anderson, S.N., Vandergheynst, J.S., Upadhyaya, S.K., Jenkins, B.M., 2014. Influence of leaching pretreatment on fuel properties of biomass. Fuel Process. Technol. 128, 43–53. https://doi.org/10.1016/j.fuproc.2014.06.030.
Zevenhoven, M., Yrjas, P., Skrifvars, B.J., Hupa, M., 2012. Characterization of ash-forming matter in various solid fuels by selective leaching and its implications for fluidized-bed combustion. Energy Fuels 26, 6366–6386. https://doi.org/10.1021/ef300621j.
Zhang, H., Ma, Y., Shao, S., Xiao, R., 2017. The effects of potassium on distributions of bio-oils obtained from fast pyrolysis of agricultural and forest biomass in a fluidized bed. Appl. Energy 208, 867–877. https://doi.org/10.1016/j.apenergy.2017.09.062.
Zhang, S., Su, Y., Xu, D., Zhu, S., Zhang, H., Liu, X., 2018. Effects of torrefaction and organic-acid leaching pretreatment on the pyrolysis behavior of rice husk. Energy 149, 804–813. https://doi.org/10.1016/J.ENERGY.2018.02.110.